DOI: 10.1002/chem.200501317

Molecular Dynamics Simulations of *p-tert*-Butylcalix[4]arene with Small Guest Molecules

Saman Alavi,*[a] Nicholas A. Afagh,[a] John A. Ripmeester,[a] and Donald L. Thompson[b]

Abstract: Classical molecular dynamics simulations were used to study *p-tert*-butylcalix[4]arene inclusion compounds with xenon, nitrogen, hydrogen, methane, and sulfur dioxide guest molecules. The calixarene units were taken to be rigid and the intermolecular molecular interactions were modeled as a sum of the van der Waals interactions with parameters from the AMBER force field and electrostatic interactions. Simulations of the high-density α phase and low-density β_0 phase of *p-tert*-butylcalix[4]arene were used to test the force field. The predicted densities of the two phases were found to agree with experimental measurements at 173 K to within 5%. Simulations were performed with guests placed inside the calixarene cages of the β_0 phase. Guest–host ratios of 1:1 to 1:4 were considered. Changes in the unit-cell volume and density of the phases with the addition of guest molecules and the inclusion energies for the guests were determined. Finally, the dynamics of the guest motion inside the cages were characterized by determining the root-mean-square displacements and velocity autocorrelation functions of the xenon and nitrogen guests.

Keywords: calixarenes · host–guest systems · inclusion compounds · molecular dynamics simulations · solid-state structures

Introduction

The *p-tert*-butylcalix[4]arene (*t*BC) molecule is a cyclic polyphenol that forms inclusion compounds with a variety of guest molecules. The structure of *t*BC is shown in Figure 1. The conelike structure of *t*BC is stabilized by the planar hydrogen bonding of the OH groups at the narrow ends of the molecule. The low-density pure form of this material is the monoclinic $P2_1/n$ β_0 phase,[1,2] which has a repeat unit consisting of four layers in an ABCD pattern in the *c* direction of the unit cell, as shown in Figure 2 (see later). The open ends of the cones are loosely associated through van der Waals interactions of the *tert*-butyl groups. In the absence of guest species, the β_0 phase remains metastable at room temperature and has a density of 1.050 g cm^{-3} and a packing efficiency of 0.59 at 173 K.[2]

Upon exposure of the β_0 phase to small gas-phase molecules, such as Xe, NO, air, SO_2, N_2, O_2, H_2, and CO_2, guest–host inclusion compounds are formed in which the host lattice structure retains the $P2_1/n$ space group.[3,4] Thermogravimetric analysis of *p-tert*-butylcalix[4]arene loaded with small molecules shows that the rate of release of the gas molecules upon heating differs significantly for various guest molecules.[3] In all cases the guest molecules are retained at temperatures much higher than their boiling point, which implies they form inclusion compounds with the calixarene and are not simply physisorbed on the calixarene surface. There is some evidence that the β_0 phase can be used to separate H_2 gas from a mixture with CO_2, because, unlike carbon dioxide, the H_2 guest molecules are not retained in the calixarene phase.[4]

In a class of larger guest molecules, such as benzene, toluene, and hexane, the low-density β_0 phase incorporates guest molecules in a 1:1 guest/host ratio and recrystallizes in the tetragonal $P4/n$ space group.[2,5] The inclusion compound of toluene (guest) with *p-tert*-butylcalix[4]arene (host) was the first crystalline calixarene to be subjected to X-ray structural analysis.[5] In this class of *t*BC inclusion compounds, the open end of the cones of adjacent bilayers are staggered in comparison with the pure β_0 phase. It was initially ob-

[a] Dr. S. Alavi, N. A. Afagh, Prof. J. A. Ripmeester
Steacie Institute for Molecular Sciences (SIMS)
National Research Council of Canada
100 Sussex Dr., Ottawa, Ontario K1A 0R6 (Canada)
Fax: (+1) 613-947-2838
E-mail: saman.alavi@nrc.ca

[b] Prof. D. L. Thompson
Department of Chemistry
University of Missouri-Columbia
Columbia Missouri, 65211 (USA)

Supporting information for this article is available on the WWW under http://www.chemeurj.org/ or from the author.

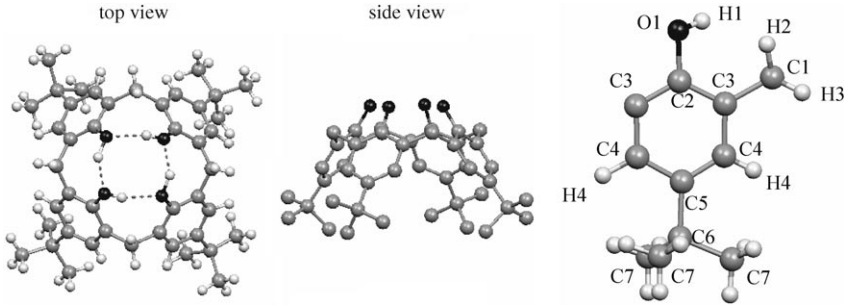

Figure 1. The top and side view of *p-tert*-butylcalix[4]arene along with the labeling of the atom types on the repeat unit of this molecule. The labels for the nine H5 atoms are not shown on the repeat unit. The black spheres represent oxygen atoms, the gray spheres carbon atoms, and the white spheres hydrogen atoms.

served that the X-ray crystal structure of the toluene–*t*BC inclusion compound was poorly refined.[6] Solid-state ^{13}C NMR spectroscopy showed that the room-temperature structure of the inclusion compound has fourfold symmetry, which is lowered to twofold symmetry as the temperature is decreased to 250 K.[7] This lowering of the symmetry has subsequently been understood as being related to the transition of the dynamics of the toluene guest molecule in the *t*BC cage from fourfold to twofold flipping, which then induces corresponding structural changes in the *t*BC cage structure.[8] X-ray crystallography analysis with Mo radiation, which is sensitive to smaller crystal domain sizes, verified this picture.[9]

Recent ab initio calculations on calixarenes and calixarene complexes have been reviewed.[10] Molecular dynamics studies of calixarene conformations,[11] cation complexation,[12,13] and liquid–liquid extraction using calixarenes[13] have been performed. Classical[14] and quantum-mechanical[15] calculations have also been performed on the effect of guest inclusion on the crystal packing of calix[4]arenes.

We decided to gain further insight into the experimental studies of small-guest inclusion compounds in calixarenes by studying their structural aspects and dynamic processes with molecular dynamics simulations. Simulations of xenon, nitrogen, hydrogen, methane, and SO_2 calixarene inclusion compounds were performed. A force field was constructed for the calixarene and evaluated by comparing its predictions for pure *p-tert*-butylcalix[4]arene α and β_0 phases with experimentally available data. Simulations with simple guest molecules inside the β_0 phase were then performed. The solid-state calixarene structure does not have pores (similar to those in zeolites) through which guest molecules diffuse. A proposed mechanism of guest-molecule motion in the calixarene phase involves shifts of the calixarene layers and the transfer of guest molecules to different cages in the shifting layers. If this mechanism is correct, the rate of diffusion of the guest molecules could depend on the magnitude of the inclusion energy in each cage. This quantity has been determined in this work and its correlation with the diffusion rates studied.

The nature of the force field and details of the molecular dynamics simulations used in the guest-free *t*BC phases and the host–guest inclusion compounds are described in the Computational Methods section. The performance of the force field in reproducing properties of the guest-free *t*BC phases is given in the Results and Discussion section along with calculated structural and dynamic properties of inclusion compounds of *t*BC with xenon, nitrogen, and hydrogen guest molecules.

Computational Methods

The *p-tert*-butylcalix[4]arene molecules were considered to be rigid in this molecular dynamics study. For the small guest molecules studied in this work, distortions of the cage structures upon guest inclusion were not observed. The initial structures of the calixarene phases used in the simulations were taken from X-ray crystallographic analyses of the appropriate pure calixarene and xenon–calixarene phases.

The intermolecular potential (V_{inter}) in the simulation were assumed to be a sum of Lennard-Jones (LJ) and electrostatic (ES) point charge potentials between atoms on different molecules, as shown in Equation (1):

$$V_{inter} = \sum_{i=1}^{N-1}\sum_{j>i}^{N}\{V^{LJ}(r_{ij}) + V^{ES}(r_{ij})\} = \sum_{i=1}^{N-1}\sum_{j>i}^{N}\left\{4\varepsilon_{ij}^{0}\left[\left(\frac{\sigma_{ij}^{0}}{r_{ij}}\right)^{12} - \left(\frac{\sigma_{ij}^{0}}{r_{ij}}\right)^{6}\right] + \frac{q_i q_j}{4\pi\varepsilon_0 r_{ij}}\right\} \quad (1)$$

The Lennard-Jones parameters ε_{ii}^{0} and σ_{ii}^{0} for the atoms of the calixarene cages were taken from the AMBER force field.[16] The combination rules, $\varepsilon_{ij}^{0} = (\varepsilon_{ii}^{0}\varepsilon_{jj}^{0})^{1/2}$ and $\sigma_{ij}^{0} = (\sigma_{ii}^{0}\sigma_{jj}^{0})^{1/2}$ were used for the Lennard-Jones potential parameters between unlike atom-type force centers *i* and *j*. The structure of the *p-tert*-butylcalix[4]arene and the atom-type assignments are shown in Figure 1 and the parameters used for the intermolecular potentials are given in Table 1. Electrostatic point charges, q_i, on atoms of the calixarene were calculated from Mulliken analysis by using the Gaussian 98 suite of programs[17] at the HF/6-31G(d) level. The large number of atoms in the calixarene unit (104) made the use of other algorithms for the determination of electrostatic point charges and higher levels of theory unwieldy. The complete set of electrostatic point charges and Cartesian coordinates of the calix[4]arene cages are given in the Supporting Information.

The Lennard-Jones parameters for the guest xenon atoms were taken from gas-phase volumetric data.[18] Nitrogen[19] and hydrogen[20] Lennard-Jones parameters and point charges were adapted from simulations of these guest molecules in clathrate hydrates. These charges were chosen to reproduce the experimental quadrupole moments of gas-phase nitrogen and hydrogen. Methane Lennard-Jones parameters were taken from the study of Murad and Gubbins[21] on dense fluid methane. The C–H bond length (1.094 Å) and electrostatic charges on the carbon and hydrogen atoms were chosen from the work of Righini et al.[22] to reproduce the calculated octupole moment of methane.[23] For sulfur dioxide, the Lennard-Jones parameters were chosen from the AMBER force field. Ko and Fink[24] used this force field along with partial charges determined by quantum-chemical calculations to reproduce the crystalline geometry of solid sulfur dioxide. We used point charges determined by the CHELPG[17,25] method and bond lengths determined at the B3LYP/6-311++G(d,p) level of theory for SO_2. The CHELPG method at this level of theory is commonly used to generate atomic electrostatic point charges for molecular dynamics calculations.

Table 1. Average atomic charges and Lennard-Jones interaction parameters used for calix[4]arene and the xenon, nitrogen, hydrogen, methane, and sulfur dioxide guests in the MD simulations. The AMBER force field atom types for the atoms of the calixarene cages are given in parentheses followed by the number of each atom type in the molecule. The numbering of the atoms is shown in Figure 1.

Atom (assignment)	q [e]	σ_{ii}^0 [Å][a]	ε_{ii}^0 [kcal mol^{-1}][a]
O1 (oh) × 4	−0.8971	3.0665	0.2104
C1 (c3) × 4	−0.3713	3.3997	0.1094
C2 (ca) × 4	+0.3239	3.3997	0.0860
C3 (ca) × 8	+0.0004	3.3997	0.0860
C4 (ca) × 8	−0.2339	3.3997	0.0860
C5 (ca) × 4	+0.0600	3.3997	0.0860
C6 (c3) × 4	−0.1314	3.3997	0.1094
C7 (c3) × 12	−0.4536	3.3997	0.1094
H1 (ho) × 4	+0.5621	0.0000	0.000
H2 (hc) × 4	+0.2188	2.6494	0.0157
H3 (hc) × 4	+0.2034	2.6494	0.0157
H4 (ha) × 8	+0.1700	2.5996	0.0150
H5 (hc) × 36	+0.1680	2.6494	0.0157
Xe	0.0000	4.0990	1.8480
N	−0.4954	3.2096	0.0809
N (cm)	+0.9908	0.0000	0.0000
H	+0.4932	0.0000	0.0000
H (cm)	−0.9864	3.0380	0.2852
C	−0.5720	3.3500	0.1017
H	+0.1430	2.6100	0.0171
S	+0.672492	3.5600	0.2000
O	−0.336246	2.9400	0.1500

[a] The intermolecular potential parameters between unlike atoms are determined from combination rules stated in the text.

Equilibrium properties of the pure calixarenes and inclusion compounds were calculated with isotropic constant pressure–constant temperature (NPT) molecular dynamics simulations by using the Nosé–Hoover thermostat–barostat algorithm[26,27] and Melchionna et al.[28] modification on the simulation cell with the DL_POLY program version 2.14.[29] The relaxation times for the thermostat and barostat were chosen as 0.1 and 1.0 ps, respectively. The equations of motion were integrated with a time step of 0.5 fs using the Verlet leapfrog scheme.[30–32] Coulombic long-range interactions were calculated by using Ewald's method,[30–32] with precision of 1×10^{-6}, and all interatomic interactions in the simulation box were calculated within a cutoff distance of $R_{cutoff} = 12.0$ Å. The simulations were carried out for a total time of 200 ps, with the first 40 ps being used for temperature-scaled equilibration. Dynamical properties were calculated with constant volume–constant energy (NVE) simulations starting from equilibrated configurations and velocities determined by using the NPT calculations. The NVE simulations were run for a total of 120 ps with 20 ps of equilibration.

Results and Discussion

Pure *p-tert*-butylcalix[4]arene has been synthesized and shows polymorphism at different temperatures. The low-temperature, high-density α phase can be crystallized from liquid tetradecane.[1,33] This solid phase has a two-layer AB repeat structure with self-included *p-tert*-butylcalix[4]arene units with one *tert*-butyl group of each unit inserted into the cone of its adjacent pair. The α phase has a $P2_1/c$ space group, a packing efficiency of 0.67, and a density of 1.157 g cm^{-3} at 173 K. The α phase has a large asymmetric unit, as determined by the complexity of its ^{13}C NMR spectrum. Upon heating to ≈250 °C, the α phase is transformed to the monoclinic $P2_1/n$ β_0 phase.[1,2] The repeat unit for this phase consists of four layers in an ABCD pattern in the c direction of the unit cell with a packing efficiency of 0.59.[2] The β_0 phase is metastable at room temperature and undergoes subtle structural rearrangements when heated and cooled.[34] The α- and β_0-phase (with xenon guests) structures are shown in Figure 2.

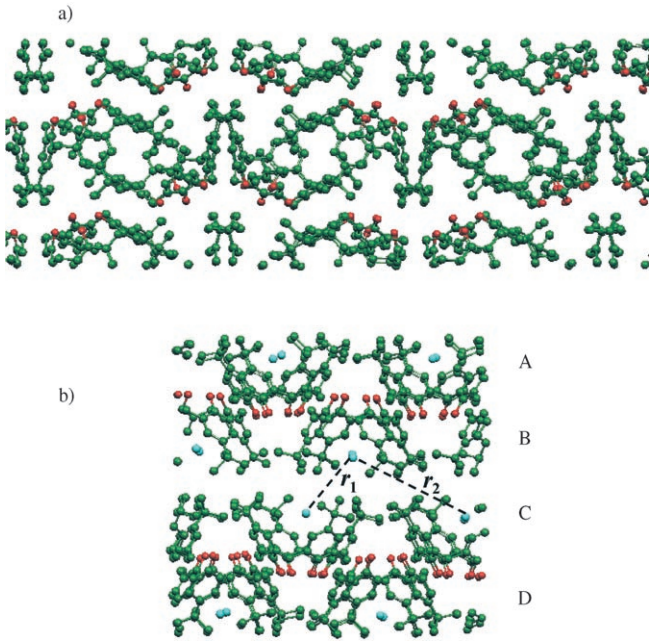

Figure 2. The structure of a) α-phase and b) β_0-phase *p-tert*-butylcalix[4]arene from X-ray diffraction data. For clarity, the hydrogen atoms are not shown. The α phase consists of AB rows of paired calixarene. The β_0 phase is made of repeating ABCD rows. The β_0 phase shown is the 1:1 xenon guest–host complex. The xenon guest atoms occupy each calixarene "cage". The smallest distances between the xenon guest atoms are shown with r_1 and r_2. Also see Figure 3. The red spheres represent oxygen atoms, the green spheres carbon atoms, and the blue spheres xenon atoms.

To test the force field, isotropic NPT simulations at ambient pressure were performed for a 3×2×2 supercell of α-phase and a 2×2×2 supercell of β_0-phase calixarenes starting from the X-ray structures at 173 K. The unit-cell volume and density were determined at each temperature. The experimentally determined density of the α phase at 173 K is 1.157 g cm^{-3},[33] and the calculated density is 1.199 g cm^{-3}, an agreement of 3%. For the β_0-phase calixarene, the experimentally determined density is 1.050 g cm^{-3},[2] and the calculated value is 1.104 g cm^{-3}, a 5% difference. In both phases, the calculations overestimate the experimental density.

A similar set of calculations was performed for inclusion compounds with xenon, nitrogen, hydrogen, methane, and sulfur dioxide guests in the β_0-phase calixarene. The calixarenes retain the β_0-phase structure in the presence of these guest molecules and the force field for the calculations was chosen to be identical to that of the pure calixarene. The fully occupied 1:1 guest/host inclusion compound for xenon

is shown in Figure 2b. Occupancies corresponding to $^3/_4$, $^2/_4$, and $^1/_4$ of the cages being filled by guests were also considered with the guest molecules distributed randomly among the cages. Experimentally, the xenon inclusion compound was found to have a 3:4 guest/host ratio.

The xenon–xenon, N_2–N_2, H_2–H_2, CH_4–CH_4 (carbon–carbon), SO_2–SO_2 (sulfur–sulfur), and SO_2–SO_2 center-of-mass radial-distribution functions (RDFs; $g(r)$) for the 1:1 host–guest solids are shown in Figure 3. For xenon, the first

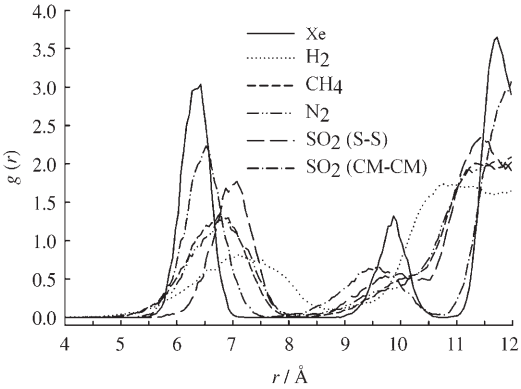

Figure 3. The Xe–Xe, N_2–N_2, H_2–H_2, CH_4–CH_4 (carbon–carbon), SO_2–SO_2 (sulfur–sulfur), and SO_2–SO_2 center-of-mass radial-distribution functions for the fully occupied 1:1 host–guest calixarene. The first two peaks for Xe and SO_2 (center-of-mass curve) correspond to the r_1 and r_2 separations shown in Figure 2b.

peak in the RDF (between 6 and 7 Å) corresponds to the separation of xenon atoms from the adjacent cages from facing rows, which is shown by r_1 in Figure 2b. The next peak (between 9 and 10.5 Å) corresponds to the separation of xenon atoms from the next nearest neighboring cages from the facing rows and is shown by r_2 in Figure 2b. In the X-ray crystal structure of this solid, the xenon atoms are disordered among three sites in each cage, which is consistent with the broad peaks of the RDF for xenon. The broad peaks of the RDF indicate dynamic motion of the xenon atoms in the cages. The RDF peaks for the N_2, H_2, and methane molecules are broader than those of Xe and have maxima spaced at larger separations. The RDF curves of methane and nitrogen are very similar. The SO_2 center-of-mass RDF is similar to that of xenon. In both cases, a distinct second peak in the RDF between 9 and 10 Å is observed that is due to strong correlations among the next nearest neighbor guests. As seen from the parameters given in Table 1, the Lennard-Jones attractions of N_2–N_2, H_2–H_2, and CH_4–CH_4 pairs are weaker than those of the Xe–Xe and SO_2–SO_2 pairs.

The dependence of the unit-cell volume and solid-state density on the fractional guest occupancy at 173 K and ambient pressure are shown in Figure 4 and the results are given in Table 2. In Figure 4, it is seen that the presence of xenon guests causes a small decrease in the unit-cell volume. The unit-cell volumes of the other guest molecules are identical within the errors of the simulation and do not show large cage-occupancy dependence. The densities of the calixarenes increase with the guest occupancy, which is due to the mass of the guest atoms incorporated in the calixarene cavities and not the variation of the unit-cell volume upon

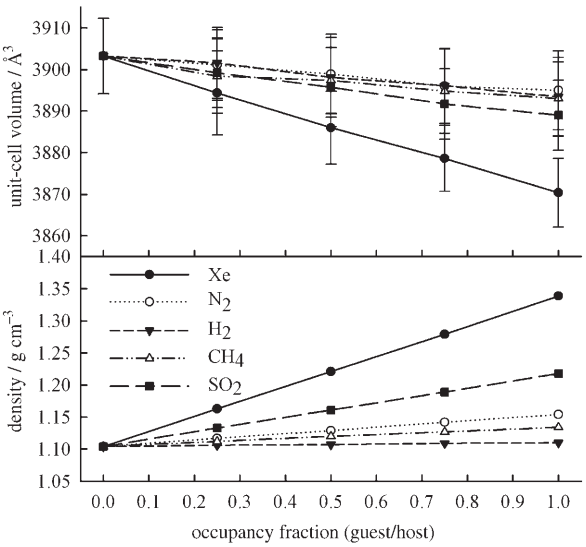

Figure 4. The variation of the unit-cell volume and density for *t*BC with xenon, nitrogen, hydrogen, methane, and sulfur dioxide guest occupancies for 1:4 to 1:1 guest/host complexes.

Table 2. Variations of the calculated unit-cell volume and density with the occupation fraction for xenon, nitrogen, hydrogen, methane, and sulfur dioxide guests in the β_0-phase calixarene at 173 K. Experimental values are given where available.

Occupation		V_{calcd} [Å^3]	V_{exptl} [Å^3]	ρ_{calcd} [g cm^{-3}]	ρ_{exptl} [g cm^{-3}]
0.00		3903.3 ± 9.1	4117	1.104 ± 0.003	1.047
Xe	0.25	3894.4 ± 10.1		1.163 ± 0.003	
	0.50	3886.0 ± 8.8		1.221 ± 0.003	
	0.75	3878.6 ± 8.0	4116	1.280 ± 0.003	1.206
	1.00	3870.4 ± 8.2		1.339 ± 0.003	
N_2	0.25	3901.1 ± 8.5		1.117 ± 0.003	
	0.50	3898.9 ± 9.6		1.129 ± 0.003	
	0.75	3896.0 ± 9.0		1.142 ± 0.003	
	1.00	3895.0 ± 9.5		1.154 ± 0.003	
H_2	0.25	3901.6 ± 8.5		1.106 ± 0.003	
	0.50	3898.1 ± 8.2		1.107 ± 0.003	
	0.75	3896.1 ± 8.9		1.109 ± 0.003	
	1.00	3893.4 ± 8.1		1.101 ± 0.003	
CH_4	0.25	3898.4 ± 8.9		1.112 ± 0.003	
	0.50	3897.4 ± 7.9		1.120 ± 0.003	
	0.75	3894.7 ± 10.1		1.127 ± 0.003	
	1.00	3893.0 ± 8.9		1.134 ± 0.003	
SO_2	0.25	3899.2 ± 8.6		1.133 ± 0.003	
	0.50	3895.8 ± 9.5		1.161 ± 0.003	
	0.75	3891.7 ± 8.5		1.189 ± 0.003	
	1.00	3889.0 ± 8.4		1.218 ± 0.003	

inclusion of the guests. The calculated density of the $^3/_4$-occupied xenon calixarene at 173 K is 1.280 g cm^{-3}, which is within 6% of the experimental value[3] of 1.206 g cm^{-3}.

The inclusion energy per unit cell, ΔE_{incl}, for the guest molecules is defined by Equation (2):

$$\Delta E_{incl} = E(\text{guest} - \text{calix}) - E(\text{calix}) - E(\text{guest}) \quad (2)$$

in which E(guest–calix) and E(calix) are the energies per unit cell of the guest–calixarene solid phase at each occupancy and the pure β_0-phase calixarene, respectively. The energy for the free guests (assumed to be an ideal gas) is E(guest) = $3nRT/2$, where n is the number of moles of guest molecules per unit cell and R is the gas constant. The inclusion energies for different occupancies are given in Table 3 and are plotted in Figure 5. The linear variation of the inclusion energy shows that up to 1:1 occupancies, there are no large-scale collective rearrangements in the structure upon guest inclusion. The values in Table 3 can be used to show that the inclusion energy per atom for xenon is the largest at −3 kcal mol^{-1}, followed by SO_2 with inclusion energy of −2 kcal mol^{-1}. For methane, nitrogen, and hydrogen guests, the inclusion energies per molecule range from −0.8 to −0.6 kcal mol^{-1}, respectively.

Table 3. Variations of the calculated inclusion energy per unit cell [kcal mol^{-1}] with occupation fraction for xenon, nitrogen, hydrogen, methane, and sulfur dioxide guests in the β_0-phase calixarene at 173 K.

Occupation	ΔE_{incl} (Xe)	ΔE_{incl} (N_2)	ΔE_{incl} (H_2)	ΔE_{incl} (CH_4)	ΔE_{incl} (SO_2)
0.25	−24.4±0.5	−6.0±0.5	−4.8±0.5	−6.2±0.5	−15.8±0.6
0.50	−47.8±0.5	−12.4±0.5	−10.3±0.5	−13.9±0.5	−31.7±0.6
0.75	−71.7±0.5	−17.7±0.5	−15.4±0.5	−20.5±0.6	−47.2±0.6
1.00	−95.9±0.5	−22.3±0.5	−20.1±0.5	−26.9±0.5	−63.4±0.6

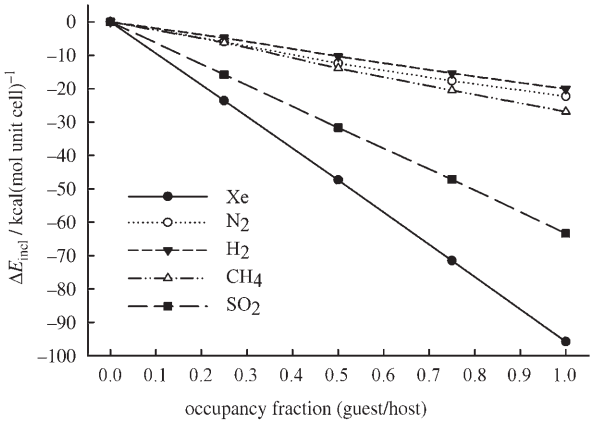

Figure 5. The variation of the inclusion energy per unit cell [kcal mol^{-1}] for *t*BC with xenon, nitrogen, hydrogen, methane, and sulfur dioxide guest occupancies for 1:4 to 1:1 guest/host complexes.

Dynamic aspects of the motion of guests in calixarene cages were studied by determining the mean-square displacement (MSD) and velocity autocorrelation function (VACF) for the center of mass of the guest molecules from NVE simulations. The MSD is defined as shown in Equation (3):

$$\Delta|\mathbf{r}(t)|^2 = \frac{1}{N}\langle \sum_{i=1}^{N} |\mathbf{r}_i(t)-\mathbf{r}_i(0)|^2 \rangle \quad (3)$$

in which $\mathbf{r}_i(t)$ is the location of the center of mass of molecule i at time t and the brackets $\langle\rangle$ represent an ensemble average. The VACF, $C_v(t)$, was calculated in dimensionless form as shown in Equation (4):

$$C_v(t) = \frac{\langle \mathbf{v}(t) \cdot \mathbf{v}(0) \rangle}{\langle \mathbf{v}(0) \cdot \mathbf{v}(0) \rangle} \quad (4)$$

in which $\mathbf{v}(t)$ is the velocity of the center of mass of the molecule. The MSD and VACF of the xenon atoms in the 1:1 guest/host calixarene are shown in Figure 6 and the corresponding curves for the center of mass of the nitrogen molecule are given in Figure 7. The small-amplitude oscillations are the most noticeable features of the two curves, and in the timescale of the simulations, the xenon and nitrogen guests are confined in the calixarene cage and do not show diffusive motion. The oscillations show that the guests undergo quasiperiodic three-dimension-

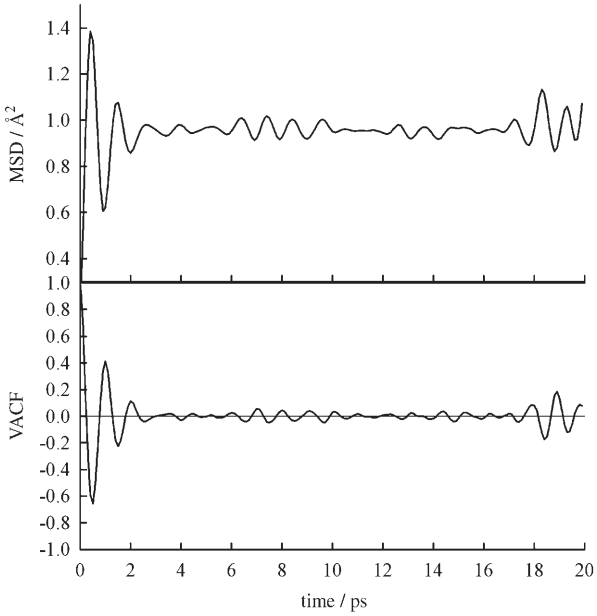

Figure 6. The mean-square displacement (MSD) and reduced velocity autocorrelation function (VACF) for the xenon guests in the 1:1 complex. The periodic motion of the guests in the cages has a time period of ≈1 ps. As expected, the oscillations of the MSD and VACF curves are out of phase.

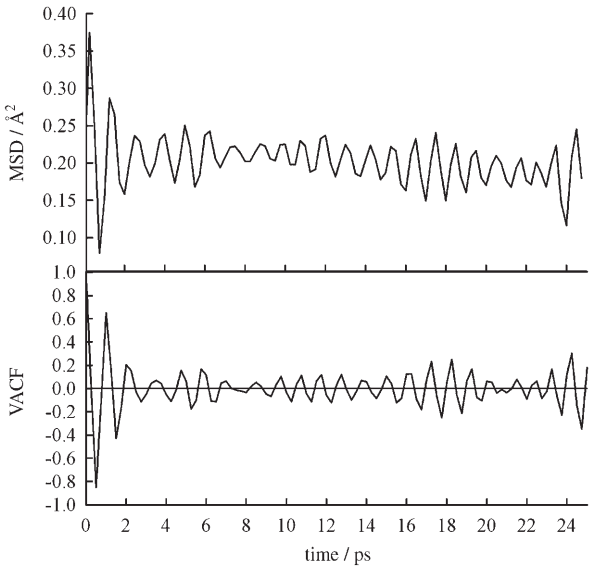

Figure 7. The mean-square displacement (MSD) and reduced velocity autocorrelation function (VACF) for the nitrogen guest center of mass in the 1:1 complex. The periodic motion of the guests in the cages has a time period of $\approx$1 ps. The oscillations of the MSD and VACF curves are out of phase.

al motions inside the cages. The VACF also shows quasiperiodic behavior centered about zero, which shows that the guests are periodically reflected by the cage walls. As expected for periodic motion of this kind, the MSD and VACF curves are effectively out of phase by $\pi/2$. The periods of the MSD and VACF motions are approximately 1 ps for the xenon atoms and lighter nitrogen molecules, as determined by direct averaging of the periods of the MSD and VACF curves in Figures 6 and 7 and Fourier analysis of these plots. The MSD and VACF curves of hydrogen, methane, and sulfur dioxide are similar to those shown in Figures 6 and 7.

The motions of guests in the cages correspond to the endohedral rattling vibrations that have been measured for different guest molecules in clathrates and thermoelectric materials.[35–37] For xenon and nitrogen guests, the rattling period of 1 ps corresponds to a frequency of 30 cm^{-1}. The rattling frequencies corresponding to the translational motion of guest molecules in clathrate hydrates and β-quinol clathrates fall in the far-infrared range of 15 to 100 cm^{-1}.[35,36] The theoretical values calculated for the guests in the calix[4]arene are consistent with this range.

Percent weight loss of the calixarene inclusion compounds as a function of temperature for NO, air, Xe, and SO_2 guests in the β_0-phase calixarene have been plotted in ref. [3]. The Xe and SO_2 guests are retained in the calixarene cages up to higher temperatures than air and NO. These plots show that guest molecules are gradually lost from the calixarene structure as the temperature is raised. The weight-loss trends shown in ref. [3] show a good correlation with the magnitude of the inclusion energies given in Table 3. This suggests that the loss of guests may involve an activated hopping process where guests jump between cages. Experimental results[38] show that the pressure dependence of the adsorption of small gas-phase molecules in the β_0-phase calixarene obeys the Langmuir adsorption isotherm.[39] The inclusion energies determined in the present work are important in quantitatively understanding this behavior. The periods of the motions of the xenon and nitrogen guests in the cages are similar ($\approx$1 ps) but their inclusion energies are different by a factor greater than three (-3 kcal mol^{-1} compared to -0.8 kcal mol^{-1}, respectively). This implies that the mechanism of diffusion is energy driven and likely occurs by site hopping,[40] which is consistent with the proposed mechanism in which calixarene planes undergo collective motions that allow guest molecules to move from cage to cage.[2,41]

Conclusions

Molecular dynamics simulations were used to study calixarene inclusion compounds with xenon, nitrogen, hydrogen, methane, and sulfur dioxide guest molecules. The AMBER force field was used to determine the intermolecular Lennard-Jones interaction parameters among atoms on different molecules. The force field was tested by comparing the calculated densities with experimental values for the high- and low-density phases of pure calixarene. The predicted results were found to be within 5% or better of experimental density values.

The unit-cell volume, density, and inclusion energy, defined in Equation (4), for different guest/host ratios were determined in this work. These quantities show linear variation with guest occupancy, which implies the absence of overall rearrangements in the solid-state structure as a result of guest inclusion. The inclusion energies per atom/molecule of xenon, sulfur dioxide, nitrogen, methane, and hydrogen are -3, -2, -0.8, -0.8, and -0.6 kcal mol^{-1}, respectively.

The mean-square displacement and velocity autocorrelation function of the xenon and nitrogen guest molecules in the calixarenes were also determined. In the timescale of the present calculations, diffusive motions of the guests were not observed. The guests undergo small-range oscillatory motions in the cages. The approximate period of these motions is $\approx$1 ps for the xenon and nitrogen guests.

Acknowledgement

This work was supported by the National Research Council of Canada. D.L.T. and S.A. wish to thank Professor Jerry L. Atwood of the Department of Chemistry, University of Missouri-Columbia, for insightful discussions. N.A.A. thanks Dr. M. Ivanov of the Theory and Computation Group of SIMS for additional financial support.

[1] E. B. Brouwer, G. D. Enright, K. A. Udachin, S. Lang, K. J. Ooms, P. A. Halchuk, J. A. Ripmeester, *Chem. Commun.* **2003**, 1416.
[2] J. L. Atwood, L. J. Barbour, A. Jerga, B. L. Schottle, *Science* **2002**, *298*, 1000.
[3] G. D. Enright, K. A. Udachin, I. L. Moudrakovski, J. A. Ripmeester, *J. Am. Chem. Soc.* **2003**, *125*, 9896.

[4] J. L. Atwood, L. J. Barbour, A. Jerga, *Angew. Chem.* **2004**, *116*, 3008; *Angew. Chem. Int. Ed.* **2004**, *43*, 2948.
[5] G. D. Andreetti, R. Ungaro, A. Pochini, *J. Chem. Soc. Chem. Commun.* **1979**, 1005.
[6] a) E. B. Brouwer, J. A. Ripmeester, G. D. Enright, *J. Incl. Phenom.* **1996**, *24*, 1; b) E. B. Brouwer, G. D. Enright, C. I. Ratcliffe, J. A. Ripmeester, K. A. Udachin in *Calixarenes 2001* (Eds.: Z. Asfari, V. Böhmer, J. Harrowfield, J. Vicens), Kluwer, Dordrecht, **2001**.
[7] a) T. Komoto, I. Ando, Y. Nakamoto, S. Ishida, *J. Chem. Soc. Chem. Commun.* **1988**, 135; b) G. A. Facey, R. H. Dubois, M. Zakrzewski, C. I. Ratcliffe, J. L. Atwood, J. A. Ripmeester, *Supramol. Chem.* **1993**, *1*, 199.
[8] E. B. Brouwer, G. D. Enright, C. I. Ratcliffe, J. A. Ripmeester, *Supramol. Chem.* **1996**, *7*, 79.
[9] G. D. Enright, E. B. Brouwer, K. A. Udachin, C. I. Ratcliffe, J. A. Ripmeester, *Acta Crystallogr. Sect. B* **2002**, *58*, 1032.
[10] J. Schatz, *Collect. Czech. Chem. Commun.* **2004**, *69*, 1169.
[11] I. Thondorf in *Calixarenes 2001* (Eds.: Z. Asfari, V. Böhmer, J. Harrowfield, J. Vicens), Kluwer, Dordrecht, **2001**, p. 280, and references therein.
[12] a) A. Ghoufi, C. Bonal, J. P. Morel, N. Morel-Desrosiers, P. Malfreyt, *J. Phys. Chem. B* **2004**, *108*, 5095; b) A. Ghoufi, C. Bonal, J. P. Morel, N. Morel-Desrosiers, P. Malfreyt, *J. Phys. Chem. B* **2004**, *108*, 11744.
[13] G. Wipff in *Calixarenes 2001* (Eds.: Z. Asfari, V. Böhmer, J. Harrowfield, J. Vicens), Kluwer, Dordrecht, **2001**, p. 312, and references therein.
[14] S. León, D. A. Leigh, F. Zerbetto, *Chem. Eur. J.* **2002**, *8*, 4854.
[15] M. I. Ogden, A. L. Rohl, J. D. Gale, *Chem. Commun.* **2001**, 1626.
[16] W. D. Cornell, P. Cieplak, C. L. Bayly, I. R. Gould, K. M. Merz, Jr., D. M. Ferguson, D. C. Spellmeyer, T. Fox, J. W. Caldwell, P. A. Kollman, *J. Am. Chem. Soc.* **1995**, *117*, 5179. See also, http://amber.scripps.edu.
[17] Gaussian 98 (Revision A.7), M. J. Frisch, G. W. Trucks, H. B. Schlegel, G. E. Scuseria, M. A. Robb, J. R. Cheeseman, V. G. Zakrzewski, J. A. Montgomery, Jr., R. E. Stratmann, J. C. Burant, S. Dapprich, J. M. Millam, A. D. Daniels, K. N. Kudin, M. C. Strain, O. Farkas, J. Tomasi, V. Barone, M. Cossi, R. Cammi, B. Mennucci, C. Pomelli, C. Adamo, S. Clifford, J. Ochterski, G. A. Petersson, P. Y. Ayala, Q. Cui, K. Morokuma, D. K. Malick, A. D. Rabuck, K. Raghavachari, J. B. Foresman, J. Cioslowski, J. V. Ortiz, B. B. Stefanov, G. Liu, A. Liashenko, P. Piskorz, I. Komaromi, R. Gomperts, R. L. Martin, D. J. Fox, T. Keith, M. A. Al-Laham, C. Y. Peng, A. Nanayakkara, C. Gonzalez, M. Challacombe, P. M. W. Gill, B. G. Johnson, W. Chen, M. W. Wong, J. L. Andres, M. Head-Gordon, E. S. Replogle, J. A. Pople, Gaussian, Inc., Pittsburgh, PA, **2001**.
[18] J. O. Hirschfelder, C. F. Curtiss, B. B. Bird, *Molecular Theory of Gases and Liquids*, Wiley, New York, **1964**.
[19] a) E. P. van Klaveren, J. P. J. Michels, J. A. Schouten, D. D. Klug, J. S. Tse, *J. Chem. Phys.* **2001**, *114*, 5745; b) E. P. van Klaveren, J. P. J. Michels, J. A. Schouten, D. D. Klug, J. S. Tse, *J. Chem. Phys.* **2001**, *115*, 10500; c) E. P. van Klaveren, J. P. J. Michels, J. A. Schouten, D. D. Klug, J. S. Tse, *J. Chem. Phys.* **2002**, *117*, 6636.
[20] S. Alavi, J. A. Ripmeester, D. D. Klug, *J. Chem. Phys.* **2005**, *122*, 024507.
[21] S. Murad, K. E. Gubbins in *Computer Modeling of Matter* (Ed.: P. Lykos), American Chemical Society, Washington D.C., **1978**, p. 62.
[22] R. Righini, K. Maki, M. L. Klein, *Chem. Phys. Lett.* **1981**, *80*, 301.
[23] I. G. John, G. B. Backsay, N. S. Hush, *Chem. Phys.* **1977**, *19*, 119; R. D. Amos, *Mol. Phys.* **1980**, *51*, 49.
[24] G. H. Ko, W. H. Fink, *Int. J. Quantum Chem.* **2003**, *95*, 830.
[25] C. M. Breneman, K. B. Wiberg, *J. Comput. Chem.* **1990**, *11*, 361.
[26] S. Nosé, *J. Chem. Phys.* **1984**, *81*, 511.
[27] W. G. Hoover, *Phys. Rev. A* **1985**, *31*, 1695.
[28] S. Melchionna, G. Ciccotti, B. L. Holian, *Mol. Phys.* **1993**, *78*, 533.
[29] DL_POLY 2.14 (Eds.: T. R. Forester, W. Smith), CCLRC, Daresbury Laboratory, **1995**.
[30] D. Frenkel, B. Smit, *Understanding Molecular Simulation*, Academic Press, San Diego, **2000**.
[31] M. P. Allen, D. J. Tildesley, *Computer Simulation of Liquids*, Oxford Science Publications, Oxford, **1987**.
[32] D. C. Rapaport, *The Art of Molecular Dynamics Simulation*, Cambridge University Press, Cambridge, **1995**.
[33] E. B. Brouwer, K. A. Udachin, G. D. Enright, J. A. Ripmeester, K. J. Ooms, P. A. Halchuk, *Chem. Commun.* **2001**, 565.
[34] J. L. Atwood, L. J. Barbour, G. O. Lloyd, P. K. Thallapally, *Chem. Commun.* **2004**, 922.
[35] J. C. Burgiel, H. Meyer, P. L. Richards, *J. Chem. Phys.* **1965**, *43*, 4291.
[36] a) J. W. Anthonsen, *Acta Chem. Scand. Ser. A* **1975**, *29*, 175; b) J. W. Anthonsen, *Acta Chem. Scand. Ser. A* **1975**, *29*, 179.
[37] G. A. Slack in *Thermoelectric Materials—New Directions and Approaches, Vol. 478* (Eds.: T. M. Tritt, G. Mahan, H. B. Lyon, Jr., M. G. Kanatzidis), Materials Research Society, Pittsburg, PA, **1997**, p. 47; G. A. Slack in *CBC Handbook of Thermoelectrics*, (Ed.: D. M. Rowe), Chemical Rubber Corporation, Boca Raton, FL, **1995**, p. 407.
[38] J. A. Ripmeester, I. L. Moudrakovski unpublished results.
[39] a) W. J. Moore, *Physical Chemistry*, Longman, London, **1986**; b) T. L. Hill, *An Introduction to Statistical Thermodynamics*, Dover, New York, **1986**.
[40] T. Ala-Nissila, R. Ferrando, S. C. Ying, *Adv. Phys.* **2002**, *51*, 949.
[41] J. W. Steed, *Science* **2002**, *298*, 976.

Received: October 21, 2005
Published online: March 10, 2006

